Biochimica et Biophysica Acta 1858 (2017) 56–63

Contents lists available at ScienceDirect

Biochimica et Biophysica Acta

journal homepage: www.elsevier.com/locate/bbabio

High photochemical trapping efficiency in Photosystem I from the red clade algae *Chromera velia* and *Phaeodactylum tricornutum*

Erica Belgio [a], Stefano Santabarbara [b,*], David Bína [c,d], Eliška Trsková [a,d], Miroslava Herbstová [c,d], Radek Kaňa [a], Giuseppe Zucchelli [b], Ondřej Prášil [a,d,**]

[a] Centre Algatech, Institute of Microbiology, Academy of Sciences of the Czech Republic, Opatovický mlýn, 379 81 Třeboň, Czech Republic
[b] Photosynthesis Research Unit, Centro per la Biologia Cellulare e Molecolare delle Piante, Via Celoria 26, 20133 Milano, Italy
[c] Biology Centre CAS, Branišovská 31, 370 05 České Budějovice, Czech Republic
[d] Faculty of Science, University of South Bohemia, Branišovská 31, 37005 České Budějovice, Czech Republic

ARTICLE INFO

Article history:
Received 2 August 2016
Received in revised form 6 October 2016
Accepted 7 October 2016
Available online 11 October 2016

Keywords:
Chromera velia
Phaeodactylum tricornutum
Red clade algae
Photosystem I
Fluorescence decay
Red spectral forms
Photochemical yield

ABSTRACT

In the present work, we report the first comparative spectroscopic investigation between Photosystem I (PSI) complexes isolated from two red clade algae. Excitation energy transfer was measured in PSI from *Chromera velia*, an alga possessing a split PsaA protein, and from the model diatom *Phaeodactylum tricornutum*. In both cases, the estimated effective photochemical trapping time was in the 15–25 ps range, i.e. twice as fast as higher plants. In contrast to green phototrophs, the trapping time was rather constant across the whole emission spectrum. The weak wavelength dependence was attributed to the limited presence of long-wavelength emitting chlorophylls, as verified by low temperature spectroscopy. As the trapping kinetics of *C. velia* PSI were barely distinguishable from those of *P. tricornutum* PSI, it was concluded that the scission of PsaA protein had no significant impact on the overall PSI functionality. In conclusion, the two red clade algae analysed here, carried amongst the most efficient charge separation so far reported for isolated Photosystems.

1. Introduction

Photosystem I (PSI) is an integral, multi-subunit, protein-cofactor complex which utilises light energy to mediate electron transfer from plastocyanin to ferredoxin (for a review, see e.g. [1–3]). The complex has two functional moieties: a central chlorophyll (Chl) *a*-binding *core*, primarily composed by two large polypeptides, PsaA and PsaB, and a peripheral antenna, displaying a high degree of variability in size, subunit and pigment compositions (reviewed in [4–5]). The *core* complex binds approximately 95 Chl *a*, six of which are involved in light-driven charge separation and comprises the terminal electron donor P_{700} (e.g. [1–3,6,7]), 15–20 β-carotene molecules, and the cofactors involved in electron transfer reactions [8,9]. The location and orientation of the *core* pigments is highly conserved between cyanobacteria and higher plants, even after 1 billion years of evolution [8–11].

Within the monophyletic "green lineage", which includes green algae and land plants, the peripheral antenna of PSI is composed of transmembrane Chl-carotenoid binding proteins. These pigment-protein complexes, collectively known as light harvesting complex I (LHCI), are arranged as a crescent-like shaped structure at one side of the monomeric core complex [4,5,10,11]. A peculiarity of plant LHCI (e.g. [12–15]), and, to less extent, of green algae LHCs (e.g. [16–18]), is a significant absorption yield in the low-energy tail (>700 nm). This has been associated with the presence of "special" Chl *a* spectral forms, the so-called "red forms", absorbing at energies lower than P_{700}. After much debate on their biological role (e.g. [19,20]), it is now generally accepted that the red forms have an important function in increasing the absorption cross-section of PSI under "shade light" conditions [21]. However, this is at the expense of a slower overall trapping rate, imposed by the "uphill" energy transfer from the red forms to the core antenna and, ultimately, to the reaction centre (e.g. [22,23]). Nevertheless, PSI trapping efficiency remains extraordinarily high (>95%, [22–25]), even in the presence of significant energy spread in its antenna. The number, localisation and spectral properties of the red forms vary considerably in different organisms (e.g. [4,5,20,26,27]). In the trimeric core of many prokaryotes, they fluoresce between 700 and 735 nm at 77 K, similarly to LHCI of higher plants [20,26]. In some green algae, like *Chlamydomonas reinhardtii*, they are less red-shifted, peaking around 715 nm (see i.e. [16–18,28,29]). Finally, most aquatic organisms belonging to the red clade division, including diatoms, cryptophytes and dinoflagellates, are normally poor in red forms content. Enrichment in the red emission tail (700–715 nm) can however

Abbreviations: PSI, Photosystem I; LHC, light harvesting complex; Chl, chlorophyll; DAS, Decay Associated Spectra; τ_{av}, (average) lifetime; FWHM, full width at half maximum.

* Corresponding author.
** Correspondence to: O. Prášil, Centre Algatech, Institute of Microbiology, Academy of Sciences of the Czech Republic, Opatovický mlýn, 379 81 Třeboň, Czech Republic.
E-mail addresses: stefano.santabarbara@cnr.it (S. Santabarbara), prasil@alga.cz (O. Prášil).

http://dx.doi.org/10.1016/j.bbabio.2016.10.002
0005-2728/

be stimulated by adaptation to far-red or low light intensities (<20 μE m^{-2} s^{-1}, [27,30]). Yet, such "conditional" red forms seem to be, at least in part, associated with the antenna of Photosystem II [31–32].

Despite the high degree of homology between PSI *cores* from different organisms, a notable exception is represented by *Chromera velia* (*C. velia*) PSI. *C. velia* is an algal symbiont of the coral reefs that displays a rather simple pigment composition, consisting of Chl *a*, isofucoxanthin-like carotenoid, violaxanthin-cycle pigments and β-carotene [33,36]. It represents an intriguing model system in many respects: it belongs to the red lineage of photosynthesis and it is therefore closely related to the intensively studied red clade diatoms; it is capable of highly efficient photosynthesis in the most various light conditions [37]; finally, it represents the evolutionary link between photosynthetic organisms and non-photosynthetic apicomplexan parasites [33–35]. Its light harvesting system appears to be phylogenetically intricate as >20 putative genes seem to encode for light harvesting complexes (LHCs) in *C. velia*. The genes have been divided into four independent groups [38], with the majority of light-harvesting complexes belonging to a cluster close to dinoflagellate and diatom LHCs [38]. Interestingly, the biochemical data [39] indicated that the LHCs associated to the PSI of *C. velia* have stronger similarities with the light harvesting complexes of red algae instead [38,40].

The photosynthetic apparatus of *C. velia* departs from the "canonical" organisation in many ways. Fundamental protein components, such as the PsaA core subunit of PSI, and the AtpB subunits of the ATPase, in the chromerid are broken into two fragments, which are independently transcribed, translated and assembled into functional PSI (Fig. 1) and ATP synthase complexes [41]. The lengths and sequences of the split PsaA fragments, PsaA1 and PsaA2, suggest that they form proteins of 4 and 7 transmembrane helixes, respectively. Comparative alignment with the crystal structure of PSI from higher plants suggested that the interface between the PsaA1 and the PsaA2 subunits is rich in Chl molecules coordinated by both segments of the split PsaA [41].

As the properties of photosynthetic complexes are mainly determined by the relative orientations and distances of their pigment complement, the question arose as to whether splitting of PsaA has an impact on the energy transfer in the *core*, thereby affecting the overall rate of photon trapping in PSI. The analysis of the excited state (fluorescence) decay represents a well-established method to investigate energy transfer and photochemical trapping in photosynthetic systems. A wide range of investigations has been already performed on PSI complexes isolated from higher plants, green algae and several cyanobacteria [7,20,22,26,42–47]. However, information concerning the PSI-LHCI complexes of red lineage algae is much more limited instead (e.g. [27,48–51]). Here, for the first time a comparative analysis based on time-resolved fluorescence spectroscopy was performed on PSI from *C. velia* and, as a control, from the diatom *Phaeodactylum tricornutum*.

In both sample investigated, the excited state decay was dominated by a lifetime of ~15–16 ps with an estimated average trapping time in the 16–25 ps range. The relatively small wavelength dependence, compared to higher plants, was attributed to the limited amount of red forms in the two algae. The average lifetimes were amongst the shortest so far reported for whole PSI-antenna preparations, yielding photochemical efficiencies exceeding 98% across the whole emission spectrum. We concluded that splitting of PsaA into two proteins in *C. velia* has no significant impact from the functional point of view. This represents yet another evidence of the overall robustness of PSI in response to perturbations of its subunits constituents.

2. Material and methods

2.1. Algal culture and PSI isolation

2.1.1. C. velia

Cultures of *C. velia* were grown in 5 l Erlenmeyer flasks at 28 °C in modified f2 medium [52] bubbled with filtered air. The cultures were illuminated by metal halide lamp (Osram Powerstar HQI 250 W/D PRO) at about 20 μmol photons m^{-2} s^{-1} in a 16/8 h light/dark regime. The purification of PSI-antenna complex was described in detail elsewhere [39]. Briefly, following several freeze-thaw cycles, the cells were broken using EmulsiFlex-C5 cell disrupter (Avestin Inc., Canada). Thylakoids were solubilized by 5% *n*-dodecyl-β-D-maltoside at a chlorophyll concentration of 1 mg ml^{-1} and fractionated using sucrose gradient centrifugation. The zone containing the PSI-antenna complexes (zone 4) was concentrated, flash-frozen in liquid nitrogen and stored at —80 °C until further use. The isolation buffer used was 50 mM MES; 5 mM $CaCl_2$; 10 mM NaCl, pH 6.5. The amount of Chl *a* per PSI RC was estimated using flash-induced absorbance change at 702 nm, using locally build instrument [53]. The extinction coefficient for PSI, determined as described in the Supporting materials, led to the estimate of ~240 Chl *a* per RC.

2.1.2. P. tricornutum. P. tricornutum

(SAG culture collection, strain 1090-1a) was grown in a modified artificial sea water f/2 + Si medium [52] aerated with sterile air in 5 l Erlenmeyer flasks maintained at 22 °C under light intensity of ~20 μmol photons m^{-2} s^{-1} provided by halogen lamp (Osram Halopar38) in a 16/8 h light/dark regime. The isolation of PSI-LHCI antenna complexes followed the procedure described in [30]. Briefly, solubilization of thylakoid membranes was achieved by 0.5% (*w*/*v*) *n*-dodecyl-β-D-maltoside (Chl *a* concentration 1 mg ml^{-1}). After ultracentrifugation, sucrose gradient zone 5 was used for PSI purification on gel filtration column and from that, fraction 1 was used for the measurements. Full characterization of this fraction has been recently described in detail [54]. Tricine buffer at

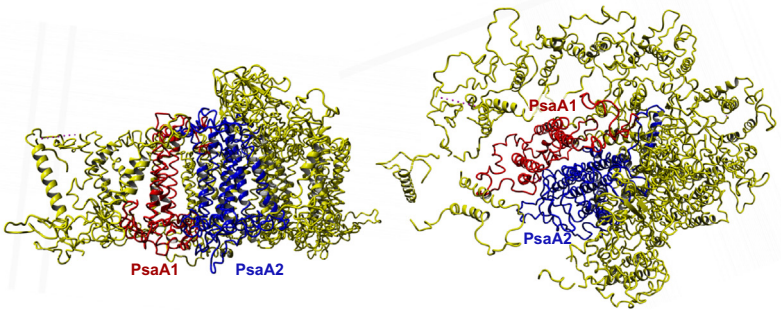

Fig. 1. Putative structure of *Chromera velia* PSI based on sequence alignment to plant supercomplex (PDB ID code 2WSC). The split of PsaA protein, peculiarity of *Chromera velia*, is shown in blue and red representing, respectively, PsaA1 and PsaA2 proteins. Left, side view; right, top view. *Re*-drawn from [41].

pH 7.5 was used throughout the isolation procedure. The estimated Chl *a*/PSI RC ratio, calculated using the extinction coefficient for PSI reported in [55] as described in Supporting Material, was about 230, in agreement with [54].

2.2. Steady-state spectroscopy

Steady state absorption and emission spectra were acquired with a laboratory assembled spectrofluorimeter, having a liquid nitrogen cooled CCD camera (Princeton Applied Research, LN/CCD-ST138), coupled to a spectrometer (SpectraPro300i), as a detector, as previously described [56,57]. Fluorescence spectra were obtained by exciting at 435 nm (full width at half maximum, FWHM, 4 nm), further filtered by a band-pass filter (Corning CS 4-96). A cut-on filter OG550 (Schott) was used to protect the CCD detector from residual straight light. Spectra were corrected for the sensitivity of the detector. Samples were diluted to a Q_y maximal optical density of 0.1 cm^{-1} to have negligible re-absorption. Low temperature measurements were performed using a flow cryostat (Oxford mod. Optistat CF) equipped with temperature control unit (ICT-503, Oxford Instruments). For room temperature measurements the samples was held at 10 °C by a circulating bath (Lauda mod. RC6-CS). For low temperature measurements the samples, held in 1 cm path-length cuvette, were suspended, immediately before cooling, in a buffer containing 70% (*w*/*v*) glycerol as a cryoprotectant to obtain transparent matrixes.

2.3. Time resolved fluorescence spectroscopy

The excited state decay kinetics were detected using a laboratory assembled Time-Correlated Single-Photon Counting set-up which has been previously described in detail [23,58]. In brief, the emission was detected by a cooled microchannel plate photomultiplier (Hamamatsu, R5916U-51). The decay kinetics were collected and stored by an integrated board (Becker & Hickl, SPC-330). The excitation is provided by a pulsed diode laser (PicoQuant 800B), centred at 632 nm (FWHM 3 nm), operating at a repetition rate of 20 MHz. The intensity was kept sufficiently weak (2 pJ/pulse) to avoid non-linear absorption processes and building-up of long lived metastable species, as shown in previous studies (e.g. [23,56,58]) employing the above described set-up. Moreover, the excitation conditions were verified on the present samples, by varying the pulse repetition rate and intensity, using neutral density filter. The kinetics were not affected by changing the average excitation flux by over one order on magnitude. The instrument response function (IRF), measured using 1,1′-Diethyl-2,2′-carbocyanine Iodide, was 110 ps FWHM, that after numerical deconvolution, allows resolving lifetimes of the order of 10 ps [58].

The samples, at an optical density 0.1 cm^{-1} at maximal absorption, were placed in a 3 mm path-length cuvette at a temperature of 10 °C. They were incubated with DCPIP (10 μM) and ascorbate (100 μM) in 25 mM Hepes, pH 7.2 to ensure photochemically open state of PSI (P_{700}).

2.4. Time resolved data analysis and parameter estimation

The excited state decay was analysed by convoluting the IRF and a decay model function, consisting in a sum of weighted exponential functions, using the global analysis approach by a laboratory developed software named *multiexp* [58,59]. The software is based on the Minuit library from CERN, distributed with a C-fortran interface as "C-minuit". Both the "C-minuit" and our Minuit-based algorithm are freely available as open-source software. The algorithm allows not only the minimization but also error analysis and determination of reduced χ^2. The output of the fit are the wavelength independent lifetime (τ_i) and their associated, wavelength dependent, pre-exponential, amplitudes ($A_i(\lambda)$) which defines the Decay Associated Spectra.

The presented DAS are the weighted mean from two to four independent purifications of PSI–LHCI, each of which was measured four times. The error bars of the DAS are the standard deviations of the weighted mean, whereas those of $(A_i(\lambda)\cdot\tau_i)$ and of the average trapping time (see below) were estimated from the propagated confidence levels.

The average trapping time (τ_{av}) was calculated from the fit solutions as $\tau_{av}(\lambda) = \sum_i A_i(\lambda)\cdot\tau_i / \sum_i A_i(\lambda)$. As previously demonstrated [56], this parameter represents the effective trapping time of the photochemistry.

3. Results

3.1. Steady state characterization at room temperature

In order to gather insight into the functional implication of the unique subunit composition of *Chromera velia* PSI, the spectroscopic properties of the supercomplex isolated from this organism were investigated and compared with those of the PSI isolated from *Phaeodactylum tricornutum*, which is a phylogenetic relative possessing "canonical" subunit composition. Fig. 2 shows the steady-state absorption and fluorescence emission spectra of the two isolated PSI-LHCI supercomplexes recorded at room temperature. The absorption shows a maximum at 678 nm in both cases, with a weak absorption tail above 700 nm. The fluorescence emission of *C. velia* PSI-LHCI is maximal at 686 nm and displays a relatively broad emission tail, from which a clear shoulder centred at about 710 nm is discernable (Fig. 2). The emission spectrum of the PSI-LHCI isolated from *P. tricornutum* shares similar characteristics with that of *C. velia*. The emission is maximal at 688 nm and displays a more asymmetric short wavelength wing with respect the chromerid supercomplex. In both samples the emission spectrum is blue-shifted with respect to higher-plant PSI supercomplex (see i.e. [23–25,42,60]). This observation is consistent with the relatively weak long-wavelength absorption tail (Fig. 2), indicating that both algae carry a limited amount of red chlorophyll (Chl) forms associated to PSI

3.2. Temperature dependence of the fluorescence emission

Fig. 3 shows the fluorescence emission spectra of PSI-LHCI supercomplexes in function of the temperature, ranging from 160 and 80 K. At the lowest temperature investigated (80 K) the isolated PSI-LHCI supercomplex of *C. velia* shows a maximal emission at 713 nm and a weak shoulder at 686 nm. The supercomplex *P. tricornutum* has, at 80 K, maximal emission at 716 nm whereas the shoulder is centred at about 688 nm

The relative intensity of the 686–688 nm and 713–716 nm bands changes as a function of temperature, with the first emission band losing intensity upon cooling with respect to the second one (Fig. 3). This behaviour is more pronounced in the *C. velia* complex, where the intensity of the 686 nm shoulder appears already substantially quenched at 120 K. The maximal emission at 713–716 nm of these complexes is about 20–25 nm blue-shifted with respect to higher plant PSI, in agreement with what previously found in diatoms [48,49,62] and some green algae, such as *C. reinhardtii* (e.g. [18,20,28,29,63]). Moreover, it is consistent with what observed at room temperature, indicating a low abundance of red Chl spectral forms in the PSI-LHCI of *C. velia* and *P. tricornutum*.

It is interesting to notice that the emission spectrum of *C. velia* is, in general, narrower than that of *P. tricornutum*, pointing at a greater inhomogeneous broadening component of the latter. Here, the presence of two sub-bands at 685 nm and 693 nm is more evident, especially at low temperature. This might be due to a slightly different composition in terms of chlorophyll forms and/or to a weaker coupling between the antenna and the relative reaction centre. In both cases, it seem to stem at the basis of the asymmetry of the short wavelength peak that is characteristic of *P. tricornutum*. The emission peak at 647 nm is due

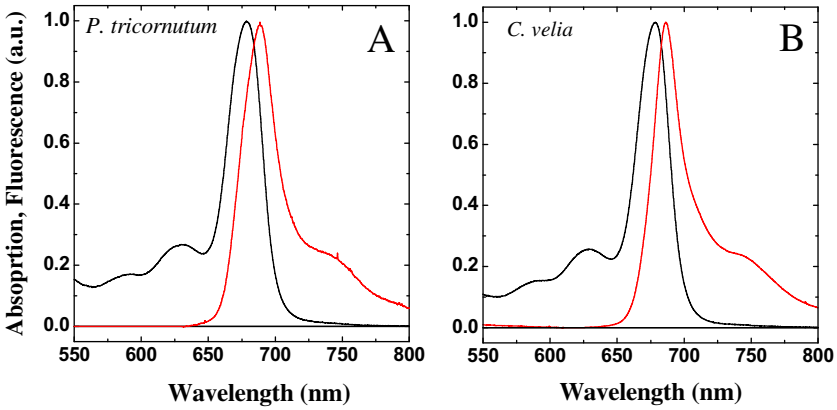

Fig. 2. Steady state absorption (black lines) and fluorescence emission (red lines) spectra of the PSI-LHCI supercomplex isolated from *P. tricornutum* (**A**) and *C. velia* (**B**) at room temperature. Excitation was at 435 nm, 5 nm full-width at half maximum for both samples.

to a small fraction of uncoupled Chl *c*, a common contaminant of these types of preparations [see i.e. 61,62]. Its contribution to the total fluorescence, however, is of negligible entity, as demonstrated by the reconstruction of the steady state spectra (see below).

3.3. Excited state dynamics at room temperature

The dynamics and efficiency of photochemical trapping in the isolated PSI-LHCI of *C. velia* and *P. tricornutum* were investigated by recording the excited state decay kinetics with picosecond temporal resolution. The kinetics were acquired in the 665–745 nm emission range, and analysed globally. Four lifetimes were necessary to describe satisfactorily the excited state decay of both *C. velia* and *P. tricornutum* PSI (see also Fig. S1 and S2 for typical distributions of residues and the wavelength-dependence of reduced χ^2_r). Fig. 4 shows the Decay Associated Spectra (DAS) of these lifetime components. Note that all the components, apart from the fastest one (15–16 ps), have been multiplied by a factor of 10 for a better visualisation.

In both PSI supercomplexes the decay is dominated by the fastest lifetime, which is characterised by values of 16 ± 2 ps, for *C. velia*, and 15 ± 1 ps, for *P. tricornutum*. These two values can be considered equal from the statistical point of view. The DAS of this component shows a maximum at 690–695 nm and displays a broad shoulder at longer wavelength, extending over the full emission window in both systems investigated. The other lifetimes, which are 176 ± 7 ps, 0.9 ± 0.1 ns and 3.7 ± 0.1 ns for the *C. velia* PS I and 180 ± 15 ps, 1.3 ± 0.1 ns and 4.3 ± 0.4 ns for the *P. tricornutum* PS I have very small associated amplitudes. These are better discernible in Fig. 5, which shows the contribution of each decay component to the fluorescence yield (which is given by the product $A_i \cdot \tau_i$).

The two longer components account for <2% of the total amplitude in *C. velia* and 4.5% in *P. tricornutum*. They have a blue-shifted DAS compared to the 15–16 ps one, peaking, in both samples, at 685 nm, as apparent from their fractional contribution to the steady state emission spectrum (Figs. 5 and S3). They are most likely associated to loosely bound antennae and/or uncoupled Chls, which are very commonly detected in isolated PSI (see i.e. [55,62,25] for an accurate discussion on this topic). However, it shall be noticed that the presence of uncoupled antennae was also suggested to occur in vivo, in diatoms cells [50]. The relative contribution of the long-lived components ($\tau > 200$ ps) is larger in the *P. tricornutum* PSI with respect to the *C. velia* supercomplex (Fig. 5), in agreement with the observation of free Chl *c* contaminant in the *P. tricornutum* preparation (Fig. 3). Moreover, this evidence, together with the analysis of low temperature emission spectra, explains the larger intensity of the blue emission wing in the steady state spectrum of *P. tricornutum* PSI (Fig. 2). This can be better appreciated from the reconstruction of the steady-state spectra presented in Supplementary Fig. S3.

The 175–180 ps lifetime component, observed in both samples, has also very low amplitude (1–4% depending on the wavelength). Yet, the origin of this component is rather ambiguous. The DAS of the 175–180 ps is blue shifted by ~5 nm with respect to the 15 ps DAS in *P. tricornutum* and by 5 nm with respect to the 16 ps DAS in *C. velia*. This suggests that it might also stem from loosely bound antenna complexes. However, the relatively fast lifetime indicates that these might be present in an aggregated form [51].

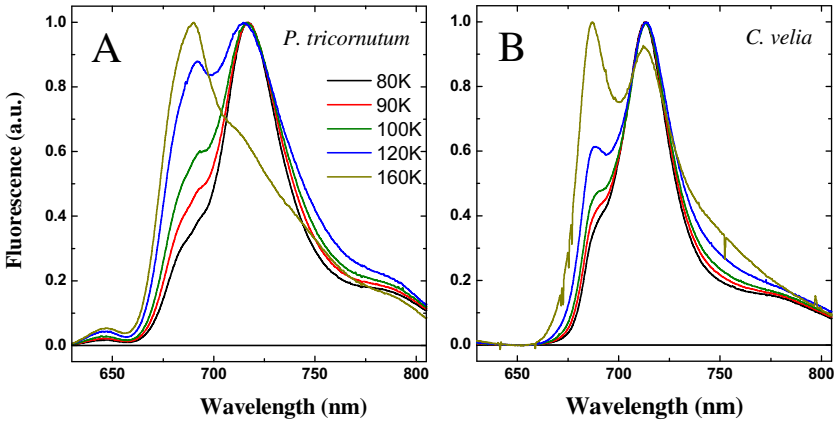

Fig. 3. Temperature dependence of the fluorescence emission spectra in the PSI-LHCI supercomplex isolated from *P. tricornutum* (**A**) and *C. velia* (**B**) in the 160-80 K interval. Each spectrum has been normalised on its maximal emission. The samples were excited a 435 nm (5 nm FWHM).

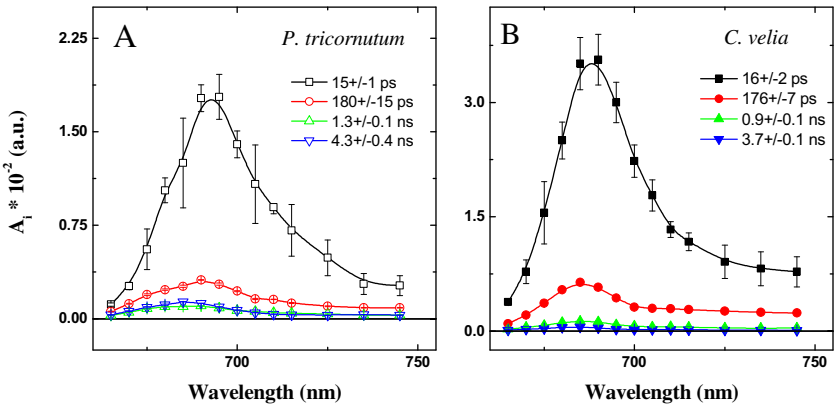

Fig. 4. Decay Associated Spectra (DAS) resulting from the global analysis of the excited state decay kinetics recorded at room temperature in the PSI-LHCI supercomplex isolated from *P. tricornutum* (**A**) and *C. velia* (**B**). The DAS are the average of between two and four independent purifications, each of which was measured four times. They have been normalised so that the total area below the whole spectrum equals unity. The error bars represent the standard deviations of the weighted mean. Note that all the components excluding the fastest one, have been multiplied by 10, in order to increase their visibility.

Nevertheless, the DAS of the 175–180 ps component displays relatively higher intensity in the red emission tail (700–725 nm), especially in *C. velia* (Fig. 4). This points at a possible contribution of slow energy transfer processes associated to moderately red-shifted Chl forms. These could be present in a fraction of the LHCI complexes which, although bound to the PSI core, exhibit a relatively slow energy transfer to the reaction centres, as already proposed for the PSI-LHCI supercomplex of *C. reinhardtii* [43,64]. Otherwise, as suggested by time resolved measurements at 17 K in the PSI-LHCI supercomplex of the diatom *Chaetocerors gracilis*, the 175–180 ps component can be associated to slow energy transfer from the redmost Chl form of the core antenna [48]. In any case, we stress the very small amplitude of these components at room temperature (Fig. 4) with respect to what observed in the previous investigation performed at 17 K [48].

3.4. Photochemical trapping efficiency

The average fluorescence lifetime, τ_{av}, calculated from the DAS and the lifetimes presented in Fig. 3, provides a reliable estimation of the *effective* photochemical trapping time [22]. Whereas the two longest lifetimes can be safely neglected from estimation of τ_{av}, the presence of the 175 ± 15 ps component might play a role despite its weak amplitude. When the 175–180 ps component is neglected from the computations, τ_{av} in both complexes coincides with the fastest decay lifetime, i.e. 16 ± 2 ps for *C. velia* and 15 ± 1 ps for *P. tricornutum*. When the 175–180 ps components are included in the calculations instead, τ_{av} varies, depending on the emission wavelength, from 18.5 to 21 ps for the *C. velia* and from 17.4 to 23 ps for the *P. tricornutum* (Fig. 6A). The increase of τ_{av} in the long emission wavelength tail is reminiscent of what was observed for the PSI-LHCI supercomplex isolated from higher plants [23–25,42,60]. In higher plants, the increase of τ_{av} in the long emission tail slows down the *effective* photochemical trapping rate to around 70 ps at these wavelengths, with respect to 20–30 ps for bulk emission wavelengths [23–25,42,60]. However, the extent of the effect observed in the complexes of *C. velia* and *P. tricornutum* is much more moderate (Fig. 6B), as τ_{av} never exceeds 25 ps in either of the samples investigated

The photochemical efficiency at the photosystem level can be conveniently evaluated considering the "overall" value of τ_{av}, which is weighted for the relative emission probabilities across the emission window considered [25]. This parameter was estimated to be 19.5 ps for *C. velia* and 18.3 ps for *P. tricornutum*, that is about two to three time faster than in the PSI-LHCI supercomplexes of higher plants and green algae e.g. [24,25,43]. Thus, irrespectively of the method employed to estimateτ_{av}, it can be concluded that the split of the PsaA core subunit in *C. velia* does not affect to any significant extent the photochemical efficiency of PSI.

As red clade algae displayed one of the fastest energy trapping so far reported for isolated Photosystem I, it can be concluded that red forms have a more profound impact on photochemistry than small local structural changes of the protein complement.

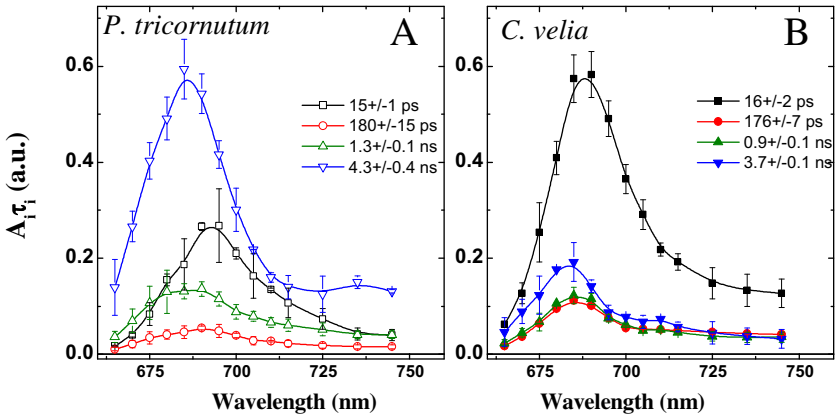

Fig. 5. Relative contributions to the steady-state emission spectra ($A_i \cdot \tau_i$) of the different decay components resulting from the global decay analysis. **A**: *P. tricornutum*; **B**: *C. velia*. The error bars are the confidence levels propagated from the standard deviations of the DAS from Fig. 4.

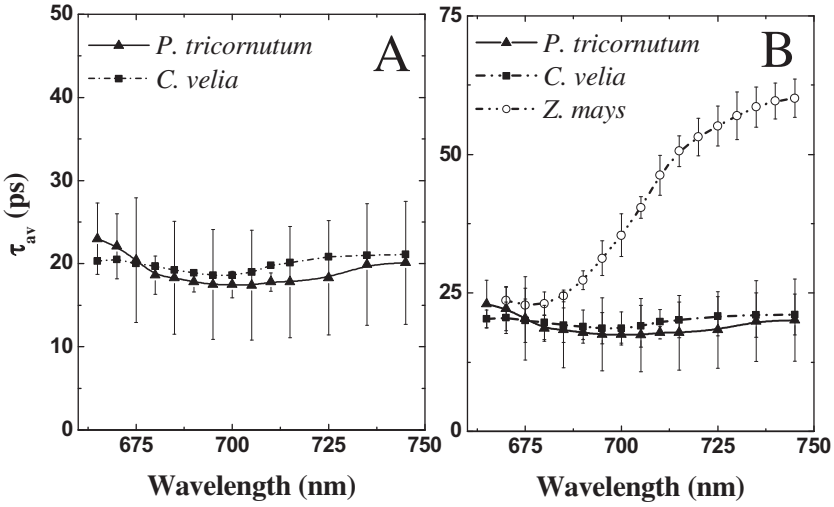

Fig. 6. Spectral dependence of the average lifetime, τ_{av}, calculated as $\Sigma Ai\tau i/\Sigma Ai$, in the isolated PSI-LHCI of *P. tricornutum* (triangles) and of *C. velia* (squares) (**A**), where the two fastest components (15 ± 1 and 180 ± 15 ps for *P. tricornutum* and 16 ± 2 and 176 ± 7 ps for *C. velia*) were considered. (**B**) Direct comparison with higher plant PSI-LHCI complex (value for plants are from [25]). The error bars were estimated from the propagated confidence levels.

4. Discussion

The analysis of excited state relaxation kinetics is a sensitive and reliable strategy to investigate energy transfer and photochemical trapping in photosynthetic systems. Therefore, this method has been widely applied to the study of PSI isolated from a broad range of organisms. These include prokaryotic cyanobacteria and eukaryotic higher plants and algae of the green lineage (reviewed in [4,5,20]).

Here for the first time we report a comparative investigation between PSI-LHCI supercomplexes from red clade algae. Low temperature fluorescence spectroscopy showed that the long-wavelength wing is similar in *C. velia* and *P. tricornutum* PSIs (Fig. 3). The red Chl forms are in both cases present in low stoichiometric amounts and also display a limited red-shift with respect to the bulk. This is in agreement with what previously observed in PSI-LHCI preparation from *P. tricornutum* [55,62] and from a different diatom, *Chaetoceros gracilis* [48]. Interestingly, the low abundance of red antenna Chls appears to be a rather common feature of most marine phytoplankton, perhaps with the exception of some cyanobateria in brackish environment (O. Prášil, unpublished data).

The excited state decay of the investigated red clade algae PSIs is remarkably fast. It is dominated by a lifetime in the order of 15–16 ps, which is in good agreement with the dominant trapping component observed in the *core* of higher plants [20,23,51,60,65], cyanobacteria (e.g. [20,45,46,66]) green algae [47,64] and diatoms [48–51]. Similar values were found for PSI isolated from *Chaetoceros gracilis* measured at 17 K [48]. The principal difference with respect to the previous study is that a faster decay component of ~5 ps was resolved in the isolated PSI of *C. gracilis*. This is likely too fast or small in amplitude to be detected by our instrumental set-up. Yet, components characterised by lifetimes in the order of 4–8 ps, are commonly detected in PSI when employing steak camera detection (e.g. [4,20] for reviews) which posses a higher temporal resolution. The fast components generally reflect energy transfer, rather than trapping, processes [4]. Therefore they have a minor impact on the estimation of the effective photochemical trapping time.

It is worth comparing our results with those previously obtained for PSI in vivo. A single component of either 50 or 75 ps has been previously retrieved for PSI on the basis of whole cell measurements of *Cyclotella meneghiniana* [50,51]. The most obvious explanation for the discrepancy with the present results resides on differences in the structural organisation of the supercomplex in the native environment. Loosely bound antenna complexes in vitro, might still be present and connected in the in vivo situation. Moreover, energy "spillover" from PSII to PSI would further increase the *effective* PSI cross-section, thus lengthening the relative lifetime. On the other hand, it cannot be excluded that the 50–74 ps component may contain a contribution from PSII. Indeed, the limited amount of red Chl forms makes it more difficult to disentangle unequivocally PSI from PSII in red clade algae than in higher plants.

The only fluorescence decay study on a PSI-LHCI supercomplex isolated from a common ancestor of *C. velia* and *P. tricornutum*, was performed on the complex of the red alga *Galderia sulphuraria* [67]. Its room temperature decay was described by one main lifetime component of 49 ps. The reason for the slower kinetics can be attributed to the increased antenna size of the *G. sulphuraria* PSI. This supercomplex binds 7–9 LHCI per RC, according to electron microscopy data, with respect to the 4 LHCI complexes per RC found in *C. velia* [39] and *P. tricornutum* [54]. Although thermophilic acidophilic red algae might be thought of as an aberrant group, that is not actually relevant to PSI evolution in secondary endosymbionts, it is still interesting to notice that both its descendants *C. velia* and *P. tricornutum* converged towards a faster photochemical trapping.

The very high photochemical efficiency of both *C. velia* and *P. tricornutum* PSI was demonstrated from the calculation of the average excited state decay lifetime (τ_{av}), which is a robust indicator of the photochemical trapping time. In the two supercomplexes isolated from red clade algae, the value of τ_{av} varied between 15 and 23 ps. These values fall on the fastest edge of the spread of trapping times previously reported for PSI core complexes [20,46] and even more so, for whole PSI-LHCI supercomplexes [4,5,20]. Moreover, τ_{av} displayed a much weaker emission wavelength dependence with respect to what observed in land plants. The marked wavelength dependence of τ_{av} in PSI-LHCI was, in higher plants, associated to the presence of long-wavelength chlorophyll emission forms, bound to the LHCI antenna [22–25]. Since the red forms absorb and emit at longer wavelength than the reaction centre, they impose a kinetic bottleneck to energy trapping, due to the uphill (energetically unfavourable) energy transfer to the reaction centre. In the case of *C. velia* and *P. tricornutum* the long-wavelength forms associated to the PSI-LHCI supercomplex are much less red-shifted than in the higher plants and appear to be in lower stoichiometric abundance. This, in turn, would limit the kinetic bottleneck for energy transfer, resulting in overall faster and less emission-wavelength-dependent values ofτ_{av} (Fig. 6). The presence of Chl red-forms in PSI external antenna has been suggested to play a major role in increasing the photosystem absorption capacity under shading conditions by leaves canopies [21], a situation which is often encountered in land plants ecological environments. Yet, severe light shading by algal culture, leading to far-red enrichment, is a much rarer situation for aquatic organisms,

that likely manifests only in the occasion of seasonal culture blooms or in peculiar ecological niches. This, together with significant absorption of far-red light photons by the water column [68] might explain both the relatively low abundance of red forms of most aquatic photosynthetic organisms and also why some red clade algae, like *Chromera velia*, have developed clever strategies for conditional synthesis of red forms, only under low light conditions [31].

In conclusion, the results obtained here indicate clearly that split of PsaA into two separate proteins does not decrease PSI photochemical efficiency. On the contrary, even higher photochemical yield than those typically reported for higher plants and green algae were estimated in the PSI isolated from both red clade algae investigated (see Fig. S4). We interpret this outstanding photochemical trapping efficiencies, as being associated to the strong reduction of energy migration bottlenecks linked to the presence of red spectral forms.

The physiological reason for the fast PSI of *P. tricornutum* and *C. velia* (about 3 times faster than higher plants), is open to speculations. It has been shown that *C. velia* efficiently acclimates to changing irradiance by stimulating photorespiration and non-photochemical quenching, thus avoiding any measurable photo-inhibition [37]. A fast PSI might be involved in alternative cyclic flow of electrons providing extra ATP or in oxygen-consuming reactions (i.e. Mehler reactions) that maintain high rates of RuBisCo type II in *C. velia* (see discussion in [37]).

In any case, the very high efficiency observed in the PSI of *C. velia*, which contains a split PsaA subunit, highlights the remarkable stability of the core protein scaffold, which is capable to achieve stable folding, and pigment docking, even when assembled from separate protein units. Given that PSI reaction centre has been already proven to be resilient to harsh biochemical treatments (e.g. reviews by [69,70]), alteration in its basic pigment composition [71,72] and extensive genetic manipulations (e.g. [73] and reference therein), this inherent robustness seems to be significant under evolutionary perspective. It is generally considered that the ancestral reaction centre shall resemble the homodimeric one found in heliobacteria and green sulphur bacteria. These are part of the so-called Type I reaction centre and are functionally related to oxygenic PSI (e.g. [74–76]). The relative flexibility of genes encoding for reaction centre subunits might provide the basis for the evolutionary success of photosynthetic phototrophs.

Author contributions

O.P., E.B., and S.S. designed research. E.B., S.S., D.B., E.T. and M.H. performed the experimental work. E.B., S.S., R.K., G.Z. and O.P. wrote the paper.

Transparency document

The Transparency document associated with this article can be found, in online version.

Acknowledgements

This research project was supported by The Czech Science Foundation GAČR (Grantová agentura České republiky) the Grant Agency of the Czech Republic, project GACR-14-15728S granted to O.P., and by the institutional projects Algatech Plus (MSMT LO1416) and Algamic (CZ 503 1.05/2.1.00/19.0392) from the Czech Ministry of Education, Youth and Sport. The work of D.B. and M.H. was supported by the Grantová Agentura České Republiky grant number P501/12/G055 and institutional support was from RVO: 60077344. The work of E.B., E.T. and R.K. was further supported by GACR 16-10088S granted to R.K.

Appendix A. Supplementary data

Supplementary data to this article can be found online at http://dx.doi.org/10.1016/j.bbabio.2016.10.002.

References

[1] K. Brettel, Electron transfer and arrangement of the redox cofactors in photosystem I, Biochim. Biophys. Acta Bioenerg. 1318 (1997) 322–373.
[2] K. Brettel, W. Leibl, Electron transfer in photosystem I, BBA 1507 (2001) 100–114.
[3] S. Santabarbara, P. Heathcote, M.C.W. Evans, Modelling of the electron transfer reactions in Photosystem I by electron tunnelling theory: the phylloquinones bound to the PsaA and the PsaB reaction centre subunits of PS I are almost isoenergetic to the iron-sulfur cluster F_X, Biochim. Biophys. Acta Bioenerg. 1708 (2005) 283–310.
[4] R. Croce, H. van Amerongen, Light-harvesting in photosystem I, Photosynth. Res. 116 (2013) 153–166.
[5] S. Caffarri, T. Tibiletti, R.C. Jennings, S. Santabarbara, A comparison between plant photosystem I and photosystem II architecture and functioning, Curr. Protein Pept. Sci. 15 (2014) 296–331.
[6] M.G. Müller, J. Niklas, W. Lubitz, A.R. Holzwarth, Ultrafast transient absorption studies on Photosystem I reaction centers from *Chlamydomonas reinhardtii*. 1. A new interpretation of the energy trapping and early electron transfer steps in Photosystem I, Biophys. J. 85 (2003) 3899–3922.
[7] W. Giera, V.M. Ramesh, A.N. Webber, I. van Stokkum, R. van Grondelle, K. Gibasiewicz, Effect of the P700 pre-oxidation and point mutations near A_0 on the reversibility of the primary charge separation in Photosystem I from *Chlamydomonas reinhardtii*, Biochim. Biophys. Acta 1797 (2010) 106–112.
[8] P. Jordan, P. Fromme, H.T. Witt, O. Klukas, W. Saenger, N. Krauss, Three-dimensional structure of cyanobacterial photosystem I at 2.5 A resolution, Nature 411 (2001) 909–917.
[9] A. Ben-Shem, F. Frolow, N. Nelson, Crystal structure of plant photosystem I, Nature 426 (2003) 630–635.
[10] E.J. Boekema, P.E. Jensen, E. Schlodder, J.F.L. van Breemen, H. van Roon, H.V. Scheller, J.P. Dekker, Green plant photosystem I binds light-harvesting complex I on one side of the complex, Biochemistry 40 (2001) 1029–1036.
[11] A. Busch, M. Hippler, The structure and function of eukaryotic photosystem I, Biochim. Biophys. Acta Bioenerg. 1807 (2011) 864–877.
[12] R. Croce, G. Zucchelli, F.M. Garlaschi, R. Bassi, R.C. Jennings, Excited state equilibration in the photosystem I light harvesting complex: P700 is almost isoenergetic with its antenna, Biochemistry 35 (1996) 8572–8579.
[13] R. Croce, G. Zucchelli, F.M. Garlaschi, R.C. Jennings, A thermal broadening study of the antenna chlorophylls in PSI-200, LHCI, and PSI core, Biochemistry 37 (1998) 17355–17360.
[14] E. Wientjes, R. Croce, The light-harvesting complexes of higher-plant photosystem I: Lhca1/4 and Lhca2/3 form two red-emitting heterodimers, Biochem. J. 433 (2011) 477–485.
[15] T. Morosinotto, J. Breton, R. Bassi, R. Croce, The nature of a chlorophyll ligand in Lhca proteins determines the far red fluorescence emission typical of photosystem I, J. Biol. Chem. 278 (2003) 49223–49229.
[16] K. Gibasiewicz, A. Szrajner, J.A. Ihalainen, M. Germano, J.P. Dekker, R. van Grondelle, b Characterization of low-energy chlorophylls in the PSI-LHCI supercomplex from *Chlamydomonas reinhardtii*. A site-selective fluorescence study, J. Phys. Chem. B. 109 (2005) 21180–21186.
[17] M. Mozzo, M. Mantelli, F. Passarini, S. Caffarri, R. Croce, R. Bassi, Functional analysis of Photosystem I light-harvesting complexes (Lhca) gene products of *Chlamydomonas reinhardtii*, Biochim. Biophys. Acta 1797 (2010) 212–221.
[18] F.-A. Wollman, P. Bennoun, A new chlorophyll-protein complex related to photosystem I in *Chlamydomonas reinhardii*, Biochim. Biophys. Acta 680 (1982) 352–360.
[19] H.W. Trissl, Long-wavelength absorbing antenna pigments and heterogeneous absorption bands concentrate excitons and increase absorption cross section, Photosynth. Res. 35 (1993) 247–263.
[20] B. Gobets, R. van Grondelle, Energy transfer and trapping in Photosystem I, Biochim. Biophys. Acta Bioenerg. 1507 (2001) 80–99.
[21] A. Rivadossi, G. Zucchelli, F.M. Garlaschi, R.C. Jennings, The importance of PSI chlorophyll red forms in light harvesting by leaves, Photosynth. Res. 60 (1999) 209–215.
[22] R.C. Jennings, G. Zucchelli, R. Croce, F.M. Garlaschi, The photochemical trapping rate from red spectral states in PSI–LHCI is determined by thermal activation of energy transfer to bulk chlorophylls, Biochim. Biophys. Acta Bioenerg. 1557 (2003) 91–98.
[23] E. Engelmann, G. Zucchelli, A.P. Casazza, D. Brogioli, F.M. Garlaschi, R.C. Jennings, Influence of the photosystem I-light harvesting complex I antenna domains on fluorescence decay, Biochemistry 45 (2006) 6947–6955.
[24] P. Galka, S. Santabarbara, T.T. Khuong, H. Degand, P. Morsomme, R.C. Jennings, E.J. Boekema, S. Caffarri, Functional analysis of the plant Photosystem I-light harvesting complex II supercomplex reveal that light harvesting complex II loosely bound to Photosystem II is a very efficient antenna for Photosystem I in state II, Plant Cell 24 (2012) 2963–2978.
[25] R.C. Jennings, G. Zucchelli, S. Santabarbara, Photochemical trapping heterogeneity as a function of wavelength, in plant photosystem I (PSI-LHCI), Biochim. Biophys. Acta Bioenerg. 1827 (2013) 779–785.
[26] N.V. Karapetyan, A.R. Holzwarth, M. Rögner, The photosystem I trimer of cyanobacteria: molecular organization, excitation dynamics and physiological significance, FEBS Lett. 460 (1999) 395–400.
[27] Y. Fujita, K. Ohki, On the 710 nm fluorescence emitted by the diatom *Phaeodactylum tricornutum* at room temperature, Plant Cell Physiol. 42 (2004) 392–397.
[28] F. Cho, Govindjee, Fluorescence spectra of chlorella in the 295–77 °K range, Biochim. Biophys. Acta 205 (1970) 371–378.
[29] F. Cho, Govindjee, Low-temperature (4–77 °K) spectroscopy of *Chlorella*; temperature dependence of energy transfer efficiency, Biochim. Biophys. Acta 216 (1970) 139–150.

[30] M. Herbstova, D. Bina, P. Konik, Z. Gardian, F. Vacha, R. Litvin, Molecular basis of chromatic adaptation in pennate diatom *Phaeodactylum tricornutum*, Biochim. Biophys. Acta 1847 (2015) 534–543.
[31] E. Kotabová, J. Jarešová, R. Kaňa, R. Sobotka, D. Bína, O. Prášil, Novel type of red-shifted chlorophyll *a* antenna complex from Chromera velia. I. Physiological relevance and functional connection to photosystems, BBA 1837 (2014) 734–743.
[32] A. Alboresi, C. Gerotto, S. Cazzaniga, R. Bassi, T. Morosinotto, A red-shifted antenna protein associated with photosystem II in *Physcomitrella patens*, J. Biol. Chem. 286 (2011) 28978–28987.
[33] R.B. Moore, M. Oborník, J. Janouškovec, T. Chrudimský, M. Vancová, D.H. Green, S.W. Wright, N.W. Davies, C.J.S. Bolch, K. Heimann, J. Šlapeta, O. Hoegh-Guldberg, J.M. Logsdon, D.A. Carter, A photosynthetic alveolate closely related to apicomplexan parasites, Nature 451 (2008) 959–963.
[34] M. Oborník, M. Vancová, D.H. Lai, J. Janouškovec, P.J. Keeling, J. Lukeš, Morphology and ultrastructure of multiple life cycle stages of the photosynthetic relative of apicomplexa, *Chromera velia*, Protist 162 (2011) 115–130.
[35] M. Oborník, J. Lukeš, The Organellar genomes of *Chromera* and *Vitrella*, the phototrophic relatives of apicomplexan parasites, Annu. Rev. Microbiol. 69 (2015) 129–144.
[36] E. Kotabová, R. Kaňa, J. Jarešová, O. Prášil, Non-photochemical fluorescence quenching in Chromera velia is enabled by fast violaxanthin de-epoxidation, FEBS 585 (2011) 1941–1945.
[37] A. Quigg, E. Kotabová, J. Jarešová, R. Kaňa, J. Šetlík, B. Šedivá, O. Komárek, O. Prášil, Photosynthesis in *Chromera velia* represents a simple system with high efficiency, PLoS One 7 (2012), e47036.
[38] H. Pan, J. Slapeta, D. Carter, M. Chen, Phylogenetic analysis of the light-harvesting system in *Chromera velia*, Photosynth. Res. 111 (2012) 19–28.
[39] J. Tichy, Z. Gardian, D. Bina, P. Konik, R. Litvin, M. Herbstova, A. Pain, F. Vacha, Light harvesting complexes of *Chromera velia*, photosynthetic relative of apicomplexan parasites, Biochim. Biophys. Acta 1827 (2013) 723–729.
[40] Z. Gardian, L. Bumba, A. Schrofel, M. Herbstova, J. Nebesarova, F. Vacha, Organisation of Photosystem I and Photosystem II in red alga *Cyanidium caldarium*: encounter of cyanobacterial and higher plant concepts, Biochim. Biophys. Acta 1767 (2007) 725–731.
[41] J. Janouškovec, R. Sobotka, D.H. Lai, P. Flegontov, P. Koník, J. Komenda, S. Ali, O. Prášil, A. Pain, M. Oborník, J. Lukeš, P.J. Keeling, Split photosystem protein, linear-mapping topology, and growth of structural complexity in the plastid genome of *Chromera velia*, Mol. Biol. Evol. 30 (2013) 2447–2462.
[42] R. Croce, D. Dorra, A.R. Holzwarth, R.C. Jennings, Fluorescence decay and spectral evolution in intact photosystem I of higher plants, Biochemistry 39 (2000) 6341–6348.
[43] C. Le Quiniou, L. Tian, B. Drop, E. Wientjes, I.H.M. van Stokkum, B. van Oort, R. Croce, PSI–LHCI of *Chlamydomonas reinhardtii*: increasing the absorption cross section without losing efficiency, Biochim. Biophys. Acta 1847 (2015) 458–467.
[44] C. Slavov, M. Ballottari, T. Morosinotto, R. Bassi, A.R. Holzwarth, Trap limited charge separation kinetics in higher plant photosystem I complexes, Biophys. J. 94 (2008) 3601–3612.
[45] A.R. Holzwarth, G. Schatz, H. Brock, E. Bittersmann, Energy transfer and charge separation kinetics in photosystem I: part 1: picosecond transient absorption and fluorescence study of cyanobacterial photosystem I particles, Biophys. J. 64 (1993) 1813–1822.
[46] I.H.M. van Stokkum, T.E. Desquilbet, W. van der Weij-de, C.D. van der, J.J. Snellenburg, R. van Grondelle, J.C. Thomas, J.P. Dekker, B.H. Robert, Energy transfer and trapping in red-chlorophyll-free Photosystem I from *Synechococcus WH 7803*, J. Phys. Chem. 117 (2013) 11176–11183.
[47] T.G. Owens, S.P. Webb, L. Mets, R.S. Alberte, G.R. Fleming, Antenna size dependence of fluorescence decay in the core antenna of Photosystem I. Estimates of charge separation and energy transfer rates, PNAS 84 (1987) 1532–1536.
[48] A. Yamagishi, Y. Ikeda, M. Komura, H. Koike, K. Satoh, S. Itoh, Y. Shibata, Shallow sink in an antenna pigment system of Photosystem I of a marine centric diatom, *Chaetoceros gracilis*, revealed by ultrafast fluorescence spectroscopy at 17 K, J. Phys. Chem. B 114 (2010) 9031–9038.
[49] Y. Ikeda, M. Komura, M. Watanabe, C. Minami, H. Koike, S. Itoh, Y. Kashino, K. Satoh, Photosystem I complexes associated with fucoxanthin-chlorophyll-binding proteins from a marine centric diatom, *Chaetoceros gracilis*, Biochim. Biophys. Acta 1777 (2008) 351–361.
[50] V.U. Chukhutsina, C. Büchel, H. van Amerongen, Variations in the first steps of photosynthesis for the diatom *Cyclotella meneghiniana* grown under different light conditions, Biochim. Biophys. Acta 1827 (2013) 10–18.
[51] Y. Miloslavina, I. Grouneva, P.H. Lambrev, B. Lepetit, R. Goss, C. Wilhelm, A.R. Holzwarth, Ultrafast fluorescence study on the location and mechanism of non-photochemical quenching in diatoms, Biochim. Biophys. Acta 1787 (2009) 1189–1197.
[52] R.R.L. Guillard, J.H. Ryther, Studies of marine planktonic diatoms I. *Cyclotella nana* Hustedt and *Detonula confervacea* (Cleve) gran, Can. J. Microbiol. 8 (1962) 229–239.
[53] D. Bína, R. Litvín, F. Vácha, P. Siffel, New multichannel kinetic spectrophotometer-fluorimeter with pulsed measuring beam for photosynthesis research, Photosynth. Res. 88 (2006) 351–356.
[54] D. Bína, M. Herbstová, Z. Gardian, F. Vácha, R. Litvín, Novel structural aspect of the diatom thylakoid membrane: lateral segregation of photosystem I under red-enhanced illumination, Sci. Rep. 6 (2016) 25583.
[55] T. Veith, C. Büchel, The monomeric photosystem I-complex of the diatom *Phaeodactylum tricornutum* binds specific fucoxanthin chlorophyll proteins (FCPs) as light-harvesting complexes, BBA 1767 (2007) 1428–1435.
[56] R.C. Jennings, G. Zucchelli, E. Engelmann, F.M. Garlaschi, The long-wavelength chlorophyll states of plant LHCI at room temperature: a comparison with PSI-LHCI, Biophys. J. 87 (2004) 488–497.
[57] E. Belgio, A.P. Casazza, G. Zucchelli, F.M. Garlaschi, R.C. Jennings, Band shape heterogeneity of the low-energy chlorophylls of CP29: absence of mixed binding sites and excitonic interactions, Biochemistry 49 (2010) 882–892.
[58] G. Tumino, A.P. Casazza, E. Engelmann, F.M. Garlaschi, G. Zucchelli, R.C. Jennings, Fluorescence lifetime spectrum of the plant photosystem II core complex: photochemistry does not induce specific reaction center quenching, Biochemistry 47 (2008) 10449–10457.
[59] F. Rizzo, G. Zucchelli, R.C. Jennings, S. Santabarbara, Wavelength dependence of the fluorescence emission under conditions of open and closed photosystem II reaction centres in the green alga *Chlorella sorokiniana*, Biochim. Biophys. Acta 1837 (2014) 726–733.
[60] E. Wientjes, I.H.M. van Stokkum, H. van Amerongen, R. Croce, Excitation energy transfer dynamics of higher plant Photosystem I light-harvesting complexes, Biophys. J. 100 (2011) 1372–1380.
[61] B. Lepetit, D. Volke, M. Szabó, R. Hoffmann, G. Garab, C. Wilhelm, R. Goss, Spectroscopic and molecular characterization of the oligomeric antenna of the diatom *Phaeodactylum tricornutum*, Biochemistry 46 (2007) 9813–9822.
[62] M. Juhas, C. Büchel, Properties of photosystem I antenna protein complexes of the diatom *Cyclotella meneghiniana* (2012), J. Exp. Bot. 63 (2012) 3673–3682.
[63] S. Santabarbara, G. Agostini, A.P. Casazza, C.D. Syme, P. Heathcote, F. Böhles, M.C. Evans, R.C. Jennings, D. Carbonera, Chlorophyll triplet states associated with Photosystem I and Photosystem II in thylakoids of the green alga *Chlamydomonas reinhardtii*, Biochim. Biophys. Acta 1767 (2007) 88–105.
[64] W. Giera, S. Szewczyk, M.D. McConnell, J. Snellenburg, K.E. Redding, R. van Grondelle, K. Gibasiewicz, Excitation dynamics in Photosystem I from *Chlamydomonas reinhardtii*. Comparative studies of isolated complexes and whole cells, Biochim. Biophys. Acta 1837 (2014) 1756–1768.
[65] J.A. Ihalainen, F. Klimmek, U. Ganeteg, I.H. van Stokkum, R. van Grondelle, S. Jansson, J.P. Dekker, Excitation energy trapping in photosystem I complexes depleted in Lhca1 and Lhca4, FEBS Lett. 579 (2005) 4787–4791.
[66] S. Turconi, J. Kruip, G. Schweitzer, M. Rögner, A.R. Holzwarth, Comparative fluorescence kinetics study of Photosystem I monomers and trimers from Synechocystis PCC 6803, Photosynth. Res. 1996 (49) (1996) 263–268.
[67] B. Thangaraj, C.C. Jolley, I. Sarrou, J.B. Bultema, J. Greyslak, J.P. Whitelegge, S. Lin, R. Kouřil, R. Subramanyam, E.J. Boekema, P. Fromme, Efficient light harvesting in a dark, hot, acidic environment: the structure and function of PSI-LHCI from *Galdieria sulphuraria*, Biophys. J. 100 (2011) 135–143.
[68] J.T.O. Kirk, Light and Photosynthesis in Acquatic Ecosystems, Cambridge University Press, Cambridge, UK, 1983 (9780521151757).
[69] I. Ikegami, S. Itoh, M. Iwaki, (2000) Selective extraction of antenna chlorophylls, carotenoids and quinones from photosystem I reaction center, Plant Cell Physiol. 41 (2000) 1085–1095.
[70] S. Itoh, M. Iwaki, I. Ikegami, Modification of photosystem I reaction center by the extraction and exchange of chlorophylls and quinones, Biochim. Biophys. Acta 1507 (2001) 115–138.
[71] S. Santabarbara, A.P. Casazza, K. Ali, C.K. Economou, T. Wannathong, F. Zito, K.E. Redding, F. Rappaport, S. Purton, The requirement for carotenoids in the assembly and function of the photosynthetic complexes in *Chlamydomonas reinhardtii*, Plant Physiol. 161 (2013) 535–546.
[72] J.A. Bautista, F. Rappaport, M. Guergova-Kuras, R.O. Cohen, J.H. Golbeck, J.Y. Wang, D. Béal, B.A. Diner, Biochemical and biophysical characterization of photosystem I from phytoene desaturase and zeta-carotene desaturase deletion mutants of Synechocystis sp. PCC 6803: evidence for PsaA- and PsaB-side electron transport in cyanobacteria, J. Biol. Chem. 280 (2005) 20030–20041.
[73] S. Santabarbara, B. Bullock, F. Rappaport, K.E. Redding, Controlling electron transfer between the two cofactor chains of photosystem I by the redox state of one of their components, Biophys. J. 108 (2015) 1537–1547.
[74] J.M. Olson, B.K. Pierson, Evolution of reation centres in photosynthetic prokariotes, Int. Rev. Cytol. 108 (1987) 209–248.
[75] J.M. Olson, R.E. Blankenship, Thinking about the evolution of photosynthesis, Photosynth. Res. 80 (2004) 373–386.
[76] J.F. Allen, A redox switch hypothesis for the origin of two light reactions in photosynthesis, FEBS Lett. 579 (2005) 963–968.